Studies of the myocardial uptake and excretion mechanisms of a novel ^{99m}Tc heart perfusion agent

Filipa Mendes[*],[1], Lurdes Gano[1], Célia Fernandes, António Paulo, Isabel Santos

Unidade de Ciências Químicas e Radiofarmacêuticas, Instituto Tecnológico e Nuclear, Estrada Nacional 10, 2686-953 Sacavém, Portugal

Abstract

Introduction: ^{99m}Tc-TMEOP is a novel heart perfusion radiotracer exhibiting high initial and persistent heart uptake associated with rapid blood and liver clearance. This study aimed at determining the mechanisms of myocardial localization and fast liver clearance of ^{99m}Tc-TMEOP.

Methods: Subcellular distribution of ^{99m}Tc-TMEOP was determined in excised rat heart tissue by differential centrifugation. The effect of cyclosporin A on the pharmacokinetic behaviour of ^{99m}Tc-TMEOP was evaluated by both ex vivo biodistribution and in vivo planar imaging studies.

Results: Subcellular distribution studies showed that more than 73% of ^{99m}Tc-TMEOP was associated with the mitochondrial fraction. Comparison with subcellular distribution of ^{99m}Tc-sestamibi showed no significant difference in the mitochondrial accumulation between the two tracers. Biodistribution studies in the presence of cyclosporin A revealed an increase in kidneys and liver uptake of ^{99m}Tc-TMEOP, suggesting the involvement of multidrug resistance transporters in determining its pharmacokinetic profile.

Conclusions: The heart uptake mechanism of ^{99m}Tc-TMEOP is similar to that of the other reported monocationic ^{99m}Tc cardiac agents and is associated with its accumulation in the mitochondria. Cyclosporin A studies indicate that the fast liver and kidney clearance kinetics is mediated by P-glycoprotein (Pgp), supporting the potential interest of this radiotracer for imaging Pgp function associated with multidrug-resistant tumours.

© 2012 Elsevier Inc. All rights reserved.

Keywords: Monocationic ^{99m}Tc-tricarbonyl complexes; Myocardial perfusion imaging; Subcellular distribution; Multidrug resistance

1. Introduction

The cationic ^{99m}Tc-radiopharmaceuticals ^{99m}Tc-sestamibi and ^{99m}Tc-tetrofosmin are widely used myocardial blood flow tracers. Although they possess adequate radiochemical characteristics, their biodistribution properties suffer well-known drawbacks, the most important being the high liver uptake, which can interfere in the analysis of cardiac imaging, particularly of the inferior left ventricular wall [1–5].

In the past, intense research efforts have been focused on the development of cationic ^{99m}Tc-labelled probes with improved cardiac-to-background ratios. So far, the most promising biological results were obtained with the mixed-ligand ^{99m}Tc(V)-nitrido complexes ^{99m}Tc-*N*-DBODC5, ^{99m}Tc-*N*-15C5 and ^{99m}Tc-*N*-MPO, and with the ^{99m}Tc(I)-tricarbonyl complex ^{99m}Tc-15C5-PNP [6–9], all these complexes being stabilized by chelation with a PNP-type bisphosphine ligand.

Recently, we investigated the coordination chemistry of azolyl-based ligands [10,11] with the ^{99m}Tc-tricarbonyl core and we were able to identify a new class of organometallic complexes based on tris(pyrazolyl)methane as lead structure [12,13]. This type of complexes has a cationic character and is stable both in vitro and in vivo. Furthermore, the tripodal chelators offer multiple possibilities of functionalization of lateral groups, thus making this new category of ^{99m}Tc-compounds potentially interesting as myocardial perfusion tracers. In particular, we discovered that the tricarbonyl complex *fac*-[^{99m}Tc(CO)$_3$\{k^3-HC[3,4,5-

* Corresponding author. Tel.: +351 219946196; fax: +351 219946185.
E-mail address: fmendes@itn.pt (F. Mendes).
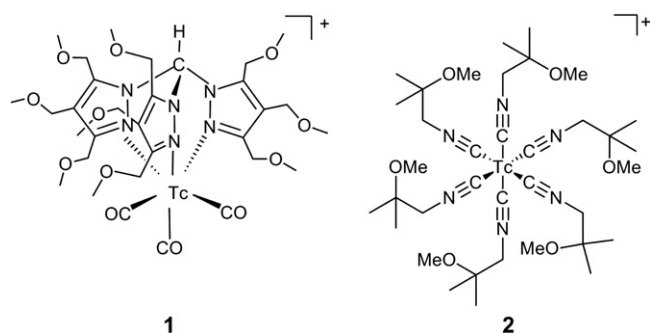[1] These authors contributed equally to this work.

Fig. 1. Structures of ^{99m}Tc-TMEOP (1) and ^{99m}Tc-sestamibi (2).

$(CH_3OCH_2)_3pz]_3\}]^+$ (Fig. 1) exhibited high heart uptake and biodistribution properties suitable for myocardial imaging [13,14].

This complex, abbreviated as ^{99m}Tc-TMEOP, has been obtained upon reaction of the neutral and tridentate nitrogen donor chelator [HC[3,4,5-$(CH_3OCH_2)_3pz]_3$ (TMEOP), with the organometallic precursor fac-[^{99m}Tc(H$_2$O)$_3$(CO)$_3$]$^+$. Although the molecular size and charge of ^{99m}Tc-TMEOP are similar to both ^{99m}Tc-sestamibi and ^{99m}Tc-tetrofosmin, the log P of ^{99m}Tc-TMEOP is lower than that of ^{99m}Tc-sestamibi (0.61±0.04 vs. 1.29±0.15) [15].

Biodistribution and cardiac pinhole-gated SPECT imaging studies in rats showed that ^{99m}Tc-TMEOP has a cardiac uptake comparable to ^{99m}Tc-sestamibi and ^{99m}Tc-tetrofosmin, but has a significantly faster liver clearance [14]. At 40 min postinjection, the heart/liver ratio of ^{99m}Tc-TMEOP is twice that of ^{99m}Tc-sestamibi and ^{99m}Tc-tetrofosmin (6.98±1.66, 2.48±0.30 and 2.66±0.40, respectively) (Fig. 2). These results are comparable with the same ratio measured at 30 min for ^{99m}Tc-N-DBODC5 (6.01±1.45) [16] and

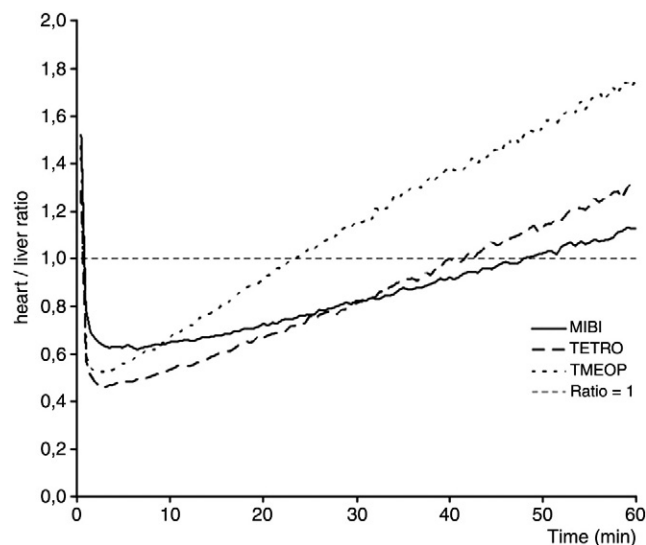Fig. 2. Heart–liver ratio calculated for ^{99m}Tc-sestamibi, ^{99m}Tc-tetrofosmin and ^{99m}Tc-TMEOP. Values are averages for six rats. MIBI=^{99m}Tc-sestamibi; TETRO=^{99m}Tc-tetrofosmin; TMEOP=^{99m}Tc-TMEOP. (Adapted from Ref. [14].)

^{99m}Tc-15C5-PNP (~5) [8,9], but inferior to that reported for ^{99m}Tc-N-MPO (12.75±3.34) [7].

Data collected so far suggest that the pharmacokinetic profile of ^{99m}Tc-TMEOP may allow high-quality imaging early after tracer injection, thereby reducing the duration of the cardiac imaging protocol and minimizing photon scattering effects [14]. Therefore, to get a better insight on the in vivo behaviour of ^{99m}Tc-TMEOP, its mechanisms of myocardial uptake and excretion have been investigated. Herein we report subcellular distribution studies of ^{99m}Tc-TMEOP performed in rat hearts, in comparison with ^{99m}Tc-sestamibi. The effect of cyclosporine A on the biodistribution properties of this new radiotracer has also been evaluated, and these results are reported in this work.

2. Materials and methods

2.1. Synthesis of ^{99m}Tc-TMEOP

A solution of [^{99m}Tc(H$_2$O)$_3$(CO)$_3$]$^+$ (1.0 ml, pH 4), obtained by reconstitution of an IsoLink kit (Covidien, Petten, the Netherlands) with generator-eluted [^{99m}TcO$_4$]$^-$, was added to a nitrogen purged vial containing 1.8 mg of TMEOP. The reaction solution was heated at 100°C, for 45 min. After cooling to room temperature, the pH was adjusted to 7 using NaOH (0.1 M). The resulting ^{99m}Tc-TMEOP was analysed by reverse-phase high-performance liquid chromatography (RP-HPLC) on a Perkin-Elmer instrument equipped with an LC pump 200 coupled to an LC 290 tunable UV/Vis detector and to a Berthold LB-507A radiometric detector. Analytical conditions were as follows: Nucleosil C18 column (10 μm, 250×4 mm); flow rate, 1 ml/min; UV detection, 254 nm; eluents, aqueous 0.1% TFA solution (A), acetonitrile (B); gradient: 0–3 min, 0% B; 3–3.1 min, 0–25% B; 3.1–9 min, 25% B; 9–9.1 min, 25–34% B; 9.1–20 min, 34–100% B; 20–22 min, 100% B; 22–22.1 min, 100–0% B; 22.1–30 min, 0% B. ^{99m}Tc-sestamibi (Cardiolite, Bristol-Myers-Squibb) was prepared and analysed according to the manufacturer's instructions.

2.2. Animal studies

All animal experiments were performed in compliance with Portuguese regulations for animal ethics and care. The animals were housed in a temperature- and humidity-controlled room with a 12-h light/12-h dark schedule and free access to food and water.

2.3. Biodistribution

Biodistribution of ^{99m}Tc-TMEOP was carried out in male Sprague-Dawley rats (6 weeks old) from IFFA CREDO, Spain. Animals were anesthetized with isoflurane inhalation (Isoflo, Abbott).

A group of animals (n=5) was intraperitoneally injected with a cyclosporin A (Cys-A) solution [16 mg/kg in 250 μl of dimethyl sulphoxide (DMSO)] 60 min before ^{99m}Tc-

TMEOP administration. As a control, a separated group of animals (n=3) was intraperitoneally injected with 250 µl of the solvent (DMSO), 60 min before ^{99m}Tc-TMEOP administration. ^{99m}Tc-TMEOP (100 µl; 4–10 MBq) was intravenously injected into the tail vein of rats, which were then sacrificed by excess anaesthesia at 0.5 and 1 h after injection. The injected activity (IA) was calculated as the difference between the measured radioactivity in the syringe before and after injection, using a curiemeter (IGC-3, Aloka, Tokyo, Japan). The organs of interest were dissected, rinsed with saline to remove excess blood, weighed and their radioactivity was measured using a gamma counter (LB2111, Berthold, Germany). The uptake in the tissues of interest was calculated as a percentage of the injected activity per gram of tissue (%IA/g). Statistical analysis of the data (t test) was done with GraphPad Prism, and the level of significance was set at .05.

2.4. Subcellular distribution studies

Subcellular distribution of ^{99m}Tc-TMEOP was evaluated in ex vivo myocardial tissue, excised 15 min after injection. Sprague-Dawley rats (n=5) were anesthetized with isoflurane and ^{99m}Tc-TMEOP or ^{99m}Tc-sestamibi administered (100 µl; 50–65 MBq). The animals were sacrificed 15 min after injection; the hearts were extracted and rapidly placed in PBS (pH=7.4) to remove residual blood. Mitochondrial isolation was performed using the Mitochondria Isolation Kit for Tissue (Pierce, Rockford, IL, USA) according to the manufacturer's instructions [17]. Briefly, the heart was grossly minced on ice with a scalpel, placed in a Dounce homogenizer with Reagent A and homogenization was achieved with ~30 strokes. Reagent C was added to the mixture which was stirred several times and finally centrifuged at 700×g for 10 min at 4°C. The resulting supernatant (A) was transferred to a tube and the resulting pellet was washed with Reagent C and centrifuged (700×g for 10 min at 4°C). The resulting pellet (Pellet I) and supernatant (B) were recovered. Supernatant B was combined with Supernatant A, and the mixed suspension was centrifuged at 3000×g for 15 min at 4°C. The resulting supernatant was recovered (Supernatant I) along with another pellet to which Reagent C was added, yielding a suspension that was then centrifuged (12,000×g for 5 min at 4°C) to give a final mitochondrial enriched pellet (Pellet II) and an additional supernatant (Supernatant II). The activity in Pellets I and II, and in Supernatants I and II was counted in a gamma counter (Berthold, Germany).

The total recovered radioactivity was calculated as the sum of radioactivity counts in Pellets I and II, and in Supernatants I and II, over the whole radioactivity measured in the isolated hearts. The percentage of radioactivity in each subcellular component was calculated as the ratio of the radioactivity count in each fraction over the total recovered radioactivity.

Malate dehydrogenase (MDH; E.C. 1.1.1.37), a mitochondrial inner matrix soluble enzyme, was used as a biomarker for assessing the percentage of mitochondrion-associated radioactivity in the various fractions. MDH activity reveals the presence of inner matrix content and, therefore, is a marker of damage to the intact mitochondrial structure. The activity of the enzyme in the different fractions was measured through a spectrophotometric rate determination according to the literature method [18].

Carbonylcyanide-m-chlorophenylhydrazone (CCCP, 5 µM) was added to the supernatants 3 min before centrifugation to evaluate the accumulation of ^{99m}Tc-complexes into intact mitochondria dispersed over each fraction. CCCP is able to uncouple the proton influx from ATP synthesis and to induce a collapse of the mitochondrial membrane potential, resulting in the release of the cationic ^{99m}Tc radiotracer from mitochondrial membrane into the supernatants.

2.5. Image acquisition

Sprague-Dawley rats (n=2 per condition) were anesthetized with isoflurane and then administered with ^{99m}Tc-TMEOP (100 µl; 4–10 MBq). Whole-body planar images of rats were obtained with a GE gamma camera connected to a Starcam 4000i computer at 30 and 60 min after injection. All the images were performed in supine position and were acquired using a 128×128 matrix.

3. Results

As previously reported, fac-[^{99m}Tc(CO)$_3${k^3-HC [3,4,5-(CH$_3$OCH$_2$)$_3$pz]$_3$}]$^+$ (^{99m}Tc-TMEOP) is obtained quantitatively and with high radiochemical purity by reacting [HC[3,4,5-(CH$_3$OCH$_2$)$_3$pz]$_3$ (TMEOP) with the organometallic precursor fac-[^{99m}Tc(OH)$_2$(CO)$_3$]$^+$, being used in the biological studies reported herein without any purification.

3.1. In vitro evaluation: subcellular localization

In order to shed light into the uptake mechanism of ^{99m}Tc-TMEOP, its subcellular distribution in rat hearts was studied. For comparison, we have also studied the subcellular distribution of ^{99m}Tc-sestamibi in parallel, in the same animal model and using the same methodology.

^{99m}Tc-TMEOP or ^{99m}Tc-sestamibi was administered, the animals were sacrificed 15 min after injection and the hearts extracted. After washing the hearts, to remove residual blood, the different subcellular fractions were separated (nuclei and cellular fragments in Pellet I, cytosol in Supernatants I and II, and mitochondria in Pellet II), using a described methodology [17].

The activity in each fraction was measured, and the radioactivity recovery was calculated based on the activity in all fractions and on the isolated hearts before homogenization. Based on three measurements, the calculated average radioactivity recovery was 80±4.5%. The radioactivity content of each fraction, expressed as a percentage of total
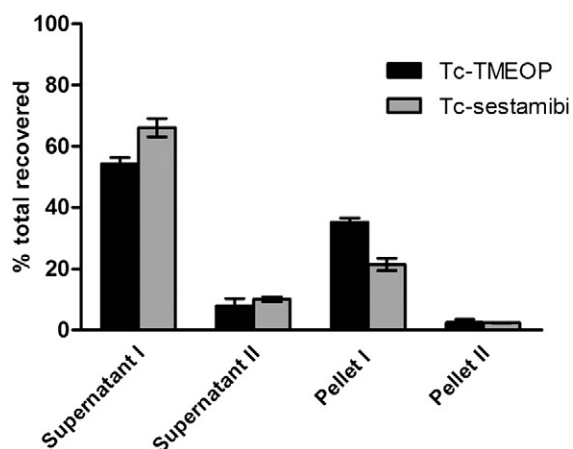
Fig. 3. Distribution of ^{99m}Tc-TMEOP and ^{99m}Tc-sestamibi in subcellular fractions obtained from rat's isolated heart (n=5).

Fig. 5. Subcellular distribution of ^{99m}Tc-TMEOP and ^{99m}Tc-sestamibi in isolated rat hearts after treatment with CCCP (5 μM).

recovered activity, was calculated, and the results are presented in Fig. 3.

Results show that both complexes have similar subcellular distributions with the major amount of radioactivity found in Supernatant I (54% for ^{99m}Tc-TMEOP and 66% for ^{99m}Tc-Sestamibi). The mitochondrial-associated activity (Pellet II) was approximately 2.56% for ^{99m}Tc-TMEOP and 2.38% for ^{99m}Tc-sestamibi.

A correlative evaluation of the presence of an inner matrix mitochondrial marker (e.g., malate dehydrogenase) in the different fractions (Supernatant I, Supernatant II, Pellet I and Pellet II) was also performed to determine any cross-contamination inherent in the isolation methodology (Fig. 4).

As shown in Fig. 4, approximately 70% to 90% of malate dehydrogenase was found in the cytosolic fraction, which also contains the largest amount of ^{99m}Tc activity (Fig. 3). These results indicate that the procedure used to separate the subcellular components damaged the mitochondrial structure, thus allowing leakage of inner matrix enzymatic content into the cytosol, as verified by other authors [19].
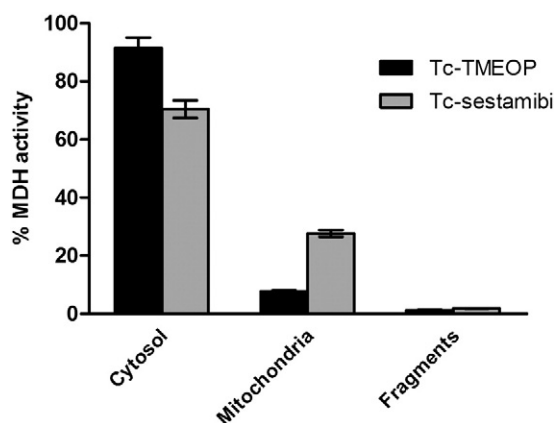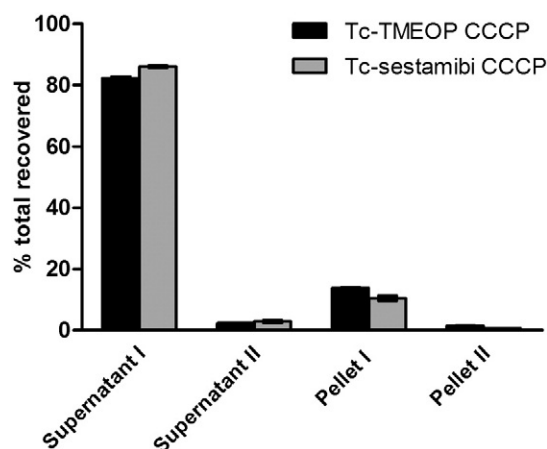
CCCP was then used to determine the radioactivity associated with intact mitochondria in Pellets I and II (containing cell fragments and mitochondria, respectively). This compound is able to uncouple the proton influx from ATP synthesis and to induce a collapse of the mitochondrial membrane potential, thus promoting the release of a cationic ^{99m}Tc radiotracer from mitochondrial pellets into the supernatant. These studies showed a significant reduction of ^{99m}Tc activity associated with the various pellets (cell fragments; nuclei in Pellet I: 21.42% vs. 10.49% for ^{99m}Tc-sestamibi and 35.22% vs. 13.8% for ^{99m}Tc-TMEOP; mitochondria in Pellet II: 2.38% vs. 0.6% for ^{99m}Tc-sestamibi and 2.56% vs. 1.47% for ^{99m}Tc-TMEOP). CCCP-releasable ^{99m}Tc activity was present in both pellets, thus revealing the presence of viable mitochondria also trapped in the cell membrane fraction (Fig. 5).

The corrected subcellular distribution of the complexes was estimated by correlating the ^{99m}Tc activity with the distribution of the markers of mitochondrial integrity.
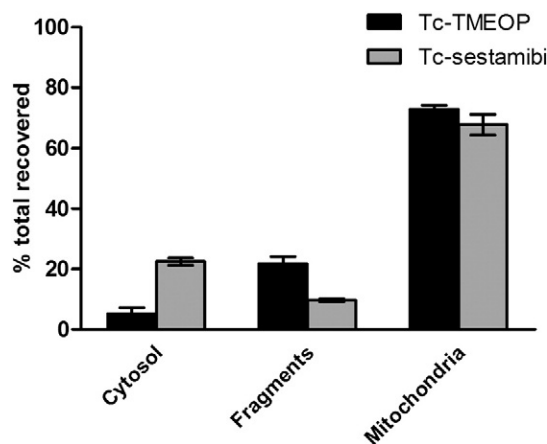

Fig. 4. Distribution of malate dehydrogenase activity in the different fractions.

Fig. 6. Corrected subcellular distribution of ^{99m}Tc-TMEOP and ^{99m}Tc-sestamibi in isolated rat's heart tissue.

Table 1
Biodistribution data of ^{99m}Tc-TMEOP (*n*=3–5) in the absence/presence of cyclosporin A

%IA/g	30 min	60 min	Cyclosporin A	
			30 min	60 min
Blood	0.15+0.05	0.32+0.16	0.21+0.10	0.22+0.09
Heart	3.90±1.00	3.70±0.90	4.40±1.40	5.20±1.90
Lung	0.90±0.10	0.80±0.40	0.95±0.15	1.20±0.20
Liver	0.24±0.09*	0.17±0.04*	2.25±0.70*	1.50±0.80*
Kidney	3.90±0.30*	3.20±0.40*	8.90±2.70*	6.40±1.10*
Intestine	3.20±0.40*	3.00±0.40	1.76±0.57*	2.50±0.80

The organ uptake is expressed as %IA/g.
  * $P<.05$.

Fig. 6 illustrates the corrected distribution of ^{99m}Tc-TMEOP and ^{99m}Tc-sestamibi.

The corrected distribution of ^{99m}Tc radioactivity was determined by assigning to the mitochondrial fraction ^{99m}Tc radioactivity associated with MDH in Supernatants I and II, or released by treatment of pellets with CCCP. Conversely, activity in Pellet II that was not affected by CCCP was attributed to the fraction containing cellular fragments, while the remaining activity was associated with the cytosolic fraction.

More than 73% of ^{99m}Tc-TMEOP and 68% of ^{99m}Tc-sestamibi were found in the mitochondria. There was no significant difference in the mitochondrial accumulation of ^{99m}Tc-TMEOP and ^{99m}Tc-sestamibi, but ^{99m}Tc-TMEOP was more present in the fragment fraction than in the cytosol, contrary to the observed for ^{99m}Tc-sestamibi.

3.2. In vivo studies: influence of cyclosporin on the biodistribution and pharmacokinetic behavior

HPLC analysis of blood and urine samples and extracts from different tissue homogenates (e.g., heart, liver, kidneys, intestine) showed that the complex ^{99m}Tc-TMEOP remains
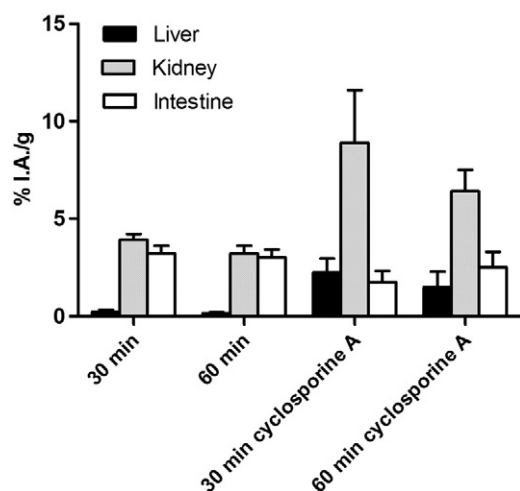

Fig. 7. Comparison of the uptake of ^{99m}Tc-TMEOP into the excretory organs in the absence or presence of cyclosporin A.

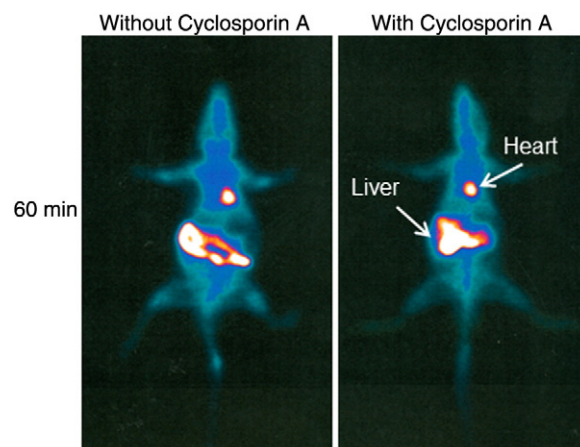Fig. 8. Planar images of rats administered with ^{99m}Tc-TMEOP (100 μl; 4–10 MBq) in the absence or presence of cyclosporin A at 60 min pi. Rats were anesthetized with isoflurane and then administered with ^{99m}Tc-TMEOP. Whole-body planar images of rats were obtained with a GE gamma camera connected to a Starcam 4000i computer at 30 and 60 min after injection. All the images were performed in supine position and were acquired using a 128×128 matrix.

intact in vivo 1 h after administration [13,14]. Therefore, metabolic transformation of ^{99m}Tc-TMEOP to more hydrophilic compounds could not be considered as an explanation for its fast liver clearance.

Hence, we investigated the existence of a possible relationship between the fast liver clearance kinetics of ^{99m}Tc-TMEOP and its potential recognition by multidrug-resistant (MDR) efflux pumps in hepatocytes by conducting biodistribution and imaging studies in rats after administration of cyclosporin A (Cys-A), a well-known wide-spectrum MDR modulator. For these experiments, cyclosporin A was intraperitoneally administered 1 h before an intravenous injection of ^{99m}Tc-TMEOP. Biodistribution data, at 30 and 60 min after ^{99m}Tc-TMEOP administration, are presented in Table 1 and Fig. 7.

Data revealed that ^{99m}Tc-TMEOP uptake increased in liver and kidneys with a concomitant lowering of its washout rate from these organs after treatment with Cys-A.

The increased liver accumulation was also apparent in planar images (Fig. 8) of the rats treated with Cys-A (16 mg/kg). On the contrary, no significant differences were observed in blood, lung and heart accumulation with respect to the control group. The intestine uptake was significantly decreased at 30 min pi within the group of animals treated with Cys-A, but these differences disappeared after 60 min.

No variation in the normal biodistribution profile of ^{99m}Tc-TMEOP was observed in rats administered intraperitoneally with DMSO 1 h before radiotracer injection.

4. Discussion

^{99m}Tc-TMEOP is a moderately lipophilic cation, which exhibits high in vivo stability, with undetectable protein

binding, being most probably distributed by the blood flow as a free cation [13,14]. We have shown that the cardiac uptake and functional pinhole gated SPECT data for ^{99m}Tc-TMEOP are comparable to those of ^{99m}Tc-sestamibi and ^{99m}Tc-tetrofosmin. Importantly, in vivo data have shown that liver clearance kinetics is much faster for ^{99m}Tc-TMEOP than for ^{99m}Tc-sestamibi and ^{99m}Tc-tetrofosmin [14]. The present study reports ongoing efforts to clarify the mechanisms responsible for the observed behaviour of this new cardiac tracer with the purpose of better understanding its potential clinical utility.

The detailed heart uptake mechanism of cationic radiotracers and the factors governing their liver clearance kinetics are not fully understood. However, several mechanistic studies suggest that both the lipophilicity and charge play a major role in the uptake and retention of ^{99m}Tc-sestamibi and other cationic radiotracers in myocytes [16]. The lipophilicity modulates the entry into the sarcolemmal and mitochondrial membranes, while the negative mitochondrial potential provides the electrochemical driving force for the radiotracers to localize in the myocyte's mitochondrial compartments [20–24]. As the myocardium has an increased mitochondrial population compared to normal tissue, lipophilic cationic radiotracers, such as ^{99m}Tc-sestamibi and ^{99m}Tc-TMEOP, tend to localize into the heart tissue. This accumulation is also visible in other mitochondrion-rich organs, such as liver and kidneys.

The subcellular distribution characteristics of ^{99m}Tc-TMEOP were compared with those of ^{99m}Tc-sestamibi using a differential centrifugation technique previously applied in the study of the subcellular myocardial localization of other cardiac tracers [19]. Only a small fraction (~2.5%) of ^{99m}Tc-TMEOP is found in the mitochondrial fraction, with the larger amount of radioactivity being found in the cytosolic fraction. Similar subcellular distribution patterns were found for ^{99m}Tc-sestamibi [19]. It has been suggested that tissue homogenization and differential centrifugation techniques may compromise mitochondrial integrity [19], thus allowing the leakage of cationic radiotracers from myocyte mitochondria. Therefore, the presence of components originating from the inner mitochondrial matrix was assessed in the cytosolic fraction with the specific enzymatic marker MDH and in the cellular fragments with CCCP, and corrected according to procedures previously described [19,25,26].

The corrected fractional distribution values (Fig. 6) clearly show that ^{99m}Tc-TMEOP and ^{99m}Tc-sestamibi are mainly localized in the mitochondrial fraction. Comparing the obtained results with the ones described in the literature in similar studies [19,25–27], we present here a somewhat different distribution of ^{99m}Tc-sestamibi (with approx. 70% in the mitochondrial fraction vs. the approx. 80% described). We believe that this disparity is not significant and is most probably due to the different methodological fractionation techniques. Moreover, the results for ^{99m}Tc-TMEOP and ^{99m}Tc-sestamibi presented were obtained in parallel experiments and there was no significant difference in their

mitochondrial accumulation. Thus, we propose that ^{99m}Tc-TMEOP, similarly to other cationic ^{99m}Tc cardiac agents, accumulates in vivo in the heart tissue due to its high mitochondrial density and through the interaction of its monopositive charge with the negative plasma and mitochondrial transmembrane potentials.

We also studied the role of P-glycoprotein (Pgp) transporter on the efflux of ^{99m}Tc-TMEOP. Pgp and other multidrug resistance–associated proteins are responsible for the efflux of a wide range of neutral and cationic substrates from organs such as the liver and the kidneys. Since it has been previously shown that ^{99m}Tc-sestamibi and ^{99m}Tc-tetrofosmin are substrates of these transporters [28–30], these agents have been used for cancer detection and monitoring of tumour MDR function.

When cyclosporin A, an MDR modulator, was administered to the animals before ^{99m}Tc-TMEOP injection, an increase on the uptake of this tracer was observed in the liver and kidneys concomitantly with a decrease of its washout rate from these organs. It is noteworthy that no significant increase in the heart uptake was observed, in accordance with the data obtained for ^{99m}Tc-N-MPO [26], but contrary to results described for ^{99m}Tc-N-DBODC5 [25], for which cyclosporin A treatment caused an increase of 30% in the heart uptake at 120 min. These results indicate that the enhanced intracellular accumulation of ^{99m}Tc-TMEOP is presumably due to Pgp inhibition by cyclosporin A. Thus, similarly to what has been previously described for the cationic tracers, ^{99m}Tc-N-DBODC5 and ^{99m}Tc-N-MPO [25], we believe that the Pgp transport (and possibly other MDR proteins) in the hepatocytes and renal brush border membrane cells could be the mechanism responsible for the rapid clearance of ^{99m}Tc-TMEOP from these excretory organs. Since liver clearance of ^{99m}Tc-TMEOP is faster than for ^{99m}Tc-sestamibi and ^{99m}Tc-tetrofosmin, this suggests that it may be more efficiently recognized by Pgp than the other two monocationic tracers, and this points to a potentially enhanced ability of ^{99m}Tc-TMEOP for imaging Pgp function associated with MDR tumours.

5. Conclusions

^{99m}Tc-TMEOP is a highly stable complex that is not metabolized in rat. Our results indicate that the heart uptake of ^{99m}Tc-TMEOP is related to its accumulation in the mitochondria due to the negative plasma and mitochondrial transmembrane potentials. The fast liver excretion of ^{99m}Tc-TMEOP seems to be mediated by Pgp, and this fact indicates that ^{99m}Tc-TMEOP may be effective for imaging Pgp function associated with MDR tumours.

Acknowledgments

References

[1] Germano G, Chua T, Kiat H, Areeda JS, Berman DS. A quantitative phantom analysis of artifacts due to hepatic activity in technetium-99m myocardial perfusion SPECT studies. J Nucl Med 1994;35:356–9.

[2] Kailasnath P, Sinusas AJ. Technetium-99m-labeled myocardial perfusion agents: Are they better than thallium-201? Cardiol Rev 2001;9:160–72.

[3] Kapur A, Latus KA, Davies G, Dhawan RT, Eastick S, Jarritt PH, et al. A comparison of three radionuclide myocardial perfusion tracers in clinical practice: the ROBUST study. Eur J Nucl Med Mol Imaging 2002;29:1608–16.

[4] Llaurado JG. The quest for the perfect myocardial perfusion indicator… still a long way to go. J Nucl Med 2001;42:282–4.

[5] Parker JA. Cardiac nuclear medicine in monitoring patients with coronary heart disease. Semin Nucl Med 2001;31:223–37.

[6] Hatada K, Riou LM, Ruiz M, Yamamichi Y, Duatti A, Lima RL, et al. ^{99m}Tc-*N*-DBODC5, a new myocardial perfusion imaging agent with rapid liver clearance: comparison with ^{99m}Tc-sestamibi and ^{99m}Tc-tetrofosmin in rats. J Nucl Med 2004;45:2095–101.

[7] Kim YS, Wang J, Broisat A, Glover DK, Liu S. Tc-99m-*N*-MPO: novel cationic Tc-99m radiotracer for myocardial perfusion imaging. J Nucl Cardiol 2008;15:535–46.

[8] Liu S. Ether and crown ether-containing cationic ^{99m}Tc complexes useful as radiopharmaceuticals for heart imaging. Dalton Trans 2007: 1183–93.

[9] Liu Z, Chen L, Liu S, Barber C, Stevenson G, Furenlid L, et al. Kinetic characterization of a novel cationic ^{99m}Tc(I)-tricarbonyl complex, ^{99m}Tc-15C5-PNP, for myocardial perfusion imaging. J Nucl Cardiol 2010;17:858–67.

[10] Santos I, Paulo A, Correia JDG. Rhenium and technetium complexes anchored by phosphines and scorpionates for radiopharmaceutical applications. In: & Kraus W, editor. Contrast Agents III — Radiopharmaceuticals — From Diagnostics to Therapeutics. Berlin: Springer; 2005, pp. 45.

[11] Garcia R, Paulo A, Santos I. Rhenium and technetium complexes with anionic or neutral scorpionates: an overview of their relevance in biomedical applications. Inorg Chim Acta 2009;362:4315–27.

[12] Maria L, Cunha S, Videira M, Gano L, Paulo A, Santos IC, et al. Rhenium and technetium tricarbonyl complexes anchored by pyrazole-based tripods: novel lead structures for the design of myocardial imaging agents. Dalton Trans 2007:3010–9.

[13] Maria L, Fernandes C, Garcia R, Gano L, Paulo A, Santos IC, et al. Tris(pyrazolyl)methane ^{99m}Tc tricarbonyl complexes for myocardial imaging. Dalton Trans 2009:603–6.

[14] Goethals LR, Santos I, Caveliers V, Paulo A, De Geeter F, Gano L, et al. Rapid hepatic clearance of ^{99m}Tc-TMEOP: a new candidate for myocardial perfusion imaging. Contrast Media Mol Imaging 2011;6:178–88.

[15] Kim YS, He Z, Hsieh WY, Liu S. Impact of bidentate chelators on lipophilicity, stability, and biodistribution characteristics of cationic ^{99m}Tc-nitrido complexes. Bioconjug Chem 2007;18:929–36.

[16] Liu S, He Z, Hsieh WY, Kim YS. Evaluation of novel cationic (99m) Tc-nitrido complexes as radiopharmaceuticals for heart imaging: improving liver clearance with crown ether groups. Nucl Med Biol 2006;33:419–32.

[17] Zhang Q, Raoof M, Chen Y, Sumi Y, Sursal T, Junger W, et al. Circulating mitochondrial DAMPs cause inflammatory responses to injury. Nature 2010;464:104–7.

[18] Bergmeyer HU. Methods of Enzymatic Analysis. New York: Verlag Academic Press; 1974.

[19] Carvalho PA, Chiu ML, Kronauge JF, Kawamura M, Jones AG, Holman BL, et al. Subcellular distribution and analysis of technetium-99m-MIBI in isolated perfused rat hearts. J Nucl Med 1992;33: 1516–22.

[20] Deutsch E, Ketring AR, Libson K, Vanderheyden JL, Hirth WW. The Noah's Ark experiment: species dependent biodistributions of cationic ^{99m}Tc complexes. Int J Radiat Appl Instrum Part B Nucl Med Biol 1989;16:191-221, 3.

[21] Platts EA, North TL, Pickett RD, Kelly JD. Mechanism of uptake of technetium-tetrofosmin: I. Uptake into isolated adult rat ventricular myocytes and subcellular localization. J Nucl Cardiol 1995;2:317–26.

[22] Younes A, Songadele JA, Maublant J, Platts E, Pickett R, Veyre A. Mechanism of uptake of technetium-tetrofosmin: II. Uptake into isolated adult rat heart mitochondria. J Nucl Cardiol 1995;2:327–33.

[23] Bolzati C, Uccelli L, Boschi A, Malago E, Duatti A, Tisato F, et al. Synthesis of a novel class of nitrido Tc-99m radiopharmaceuticals with phosphino-thiol ligands showing transient heart uptake. Nucl Med Biol 2000;27:369–74.

[24] Piwnica-Worms D, Kronauge JF, Chiu ML. Uptake and retention of hexakis (2-methoxyisobutyl isonitrile) technetium(I) in cultured chick myocardial cells. Mitochondrial and plasma membrane potential dependence. Circulation 1990;82:1826–38.

[25] Bolzati C, Cavazza-Ceccato M, Agostini S, Tokunaga S, Casara D, Bandoli G. Subcellular distribution and metabolism studies of the potential myocardial imaging agent [^{99m}Tc(N)(DBODC)(PNP5)]+. J Nucl Med 2008;49:1336–44.

[26] Kim YS, Shi J, Zhai S, Hou G, Liu S. Mechanism for myocardial localization and rapid liver clearance of Tc-99m-*N*-MPO: a new perfusion radiotracer for heart imaging. J Nucl Cardiol 2009;16: 571–9.

[27] Uccelli L, Giganti M, Duatti A, Bolzati C, Pasqualini R, Cittanti C, et al. Subcellular distribution of technetium-99m-*N*-NOEt in rat myocardium. J Nucl Med 1995;36:2075–9.

[28] Piwnica-Worms D, Chiu ML, Budding M, Kronauge JF, Kramer RA, Croop JM. Functional imaging of multidrug-resistant P-glycoprotein with an organotechnetium complex. Cancer Res 1993;53:977–84.

[29] Ballinger JR, Bannerman J, Boxen I, Firby P, Hartman NG, Moore MJ. Technetium-99m-tetrofosmin as a substrate for P-glycoprotein: in vitro studies in multidrug-resistant breast tumor cells. J Nucl Med 1996;37: 1578–82.

[30] Ballinger JR, Muzzammil T, Moore MJ. Technetium-99m-furifosmin as an agent for functional imaging of multidrug resistance in tumors. J Nucl Med 1997;38:1915–9.